



Graphene/Gold Nanoparticles Composites for Ultrasensitive and Versatile Biomarker Assay Using Single-Particle Inductively-Coupled Plasma/Mass Spectrometry

Journal:	<i>Analyst</i>
Manuscript ID	AN-ART-05-2020-001019.R1
Article Type:	Paper
Date Submitted by the Author:	05-Sep-2020
Complete List of Authors:	Xing, Yuqian; University of North Dakota Han, Juan; University of North Dakota, Chemistry Wu, Xu; University of North Dakota, Chemistry Pierce, David; University of North Dakota, Chemistry Zhao, Julia; University of North Dakota, Chemistry

1
2
3 **Graphene/Gold Nanoparticles Composites for Ultrasensitive and**
4 **Versatile Biomarker Assay Using Single-Particle Inductively-**
5 **Coupled Plasma/Mass Spectrometry**
6
7
8
9
10
11
12

13 Yuqian Xing, Juan Han, Xu Wu, David T. Pierce* and Julia Xiaojun Zhao*
14
15

16 Department of Chemistry, University of North Dakota, Grand Forks, North Dakota 58202,
17
18 United States
19
20
21

22 AUTHOR INFORMATION
23
24

25 **Co-Corresponding Authors**
26

27 julia.zhao@und.edu (J.X. Zhao)
28

29 david.pierce@und.edu (D.T. Pierce)
30
31
32
33

34 **KEYWORDS:** AuNPs, graphene oxide, ssDNA, spICP-MS, ultrasensitive assay,
35
36 **biomarker**
37

38 **ABSTRACT:**
39

40
41 An ultrasensitive and versatile assay for biomarkers has been developed using graphene/gold
42 nanoparticles (AuNPs) composites and single-particle inductively-coupled plasma/mass
43 spectrometry (spICP-MS). Thrombin was chosen as a model biomarker for this study. AuNPs
44 modified with thrombin aptamers were first non-selectively adsorbed onto the surface of
45 graphene oxide (GO) to form GO/AuNPs composites. In the presence of thrombin, the AuNPs
46 desorbed from the GO/AuNPs composites due to a conformation change of the thrombin aptamer
47 after binding with thrombin. The desorbed AuNPs were proportional to the concentration of
48
49
50
51
52
53
54
55
56
57
58
59
60

1
2
3 thrombin and could be quantified by spICP-MS. By counting the individual AuNPs in the spICP-
4 MS measurement, the concentration of thrombin could be determined. This assay achieved an
5 ultralow detection limit of 4.5 fM with a broad linear range from 10 fM to 100 pM. The method
6 also showed excellent selectivity and reproducibility when a complex protein matrix was
7 evaluated. Furthermore, the diversity and ready availability of ssDNA ligands make this method
8 a versatile new technique for ultrasensitive detection of a wide variety of biomarkers in clinical
9 diagnostics.

19 **1. Introduction**

21 Graphene oxide (GO) has been widely applied for fluorescence-based bioassays due to its unique
22 optical properties.^{1, 2} In general, it is a high-capacity energy acceptor and has played a significant
23 role as a quencher in the fluorescence resonance energy transfer (FRET) of optical bioassays.^{3, 4}
24 For instance, single-stranded DNA (ssDNA) is easily adsorbed to the GO surface because of
25 strong π - π stacking interactions between the base structure of ssDNA and the two-dimensional
26 multi-hexagonal structure of GO.⁵ The strong adsorption between GO and ssDNA, coupled with
27 the excellent quenching ability of GO provides an sensitive fluorescence platform for detecting
28 and determining the concentration of biomolecules.⁶ Two major factors determine the sensitivity
29 of DNA-sensing applications of this platform. The first factor is a target-induced DNA
30 conformational change, which results in desorption of fluorophore molecules from the GO, and
31 thus increased fluorescence signal. Since the first report by Lu *et al.* in 2009,⁶ a broad range of
32 targets including nucleotides,⁷ metal ions,⁸ proteins,⁹ enzymes,¹⁰ and other small molecules¹¹
33 have been detected using various ssDNA conformational changes with this platform.¹² The
34 second factor is the emission output based on FRET between fluorophore molecules and the GO.
35 However, the high background emission of some complex samples,¹³ photobleaching of the
36
37
38
39
40
41
42
43
44
45
46
47
48
49
50
51
52
53
54
55
56
57
58
59
60

1
2
3 fluorophores, and practical limitations of the fluorophotometers have prevented more than
4
5 incremental improvements in optical sensitivity and therefore limited achievement of sub-
6
7 picomolar detection. Thus, a better signaling method is needed to achieve these ultratrace
8
9 detection limits.

10
11
12 Two possible strategies could improve the signal output and lower the detection limits of the GO
13
14 platform. The first strategy is to introduce an amplification step in the sensing process.¹⁴ Several
15
16 of these methods have been applied for oligonucleotide amplification, such as polymerase chain
17
18 reaction and other isothermal nucleic acid amplification methods.¹⁵ However, specific enzymes
19
20 and delicate sequence design were required, diminishing the assay feasibility or versatility. The
21
22 second strategy is to utilize a more sensitive signaling scheme. A detection method can response
23
24 to ultralow amount of the target, such as electrochemical sensors and surface-enhanced Raman
25
26 spectroscopy.¹⁶⁻¹⁸ Another candidate is the inductively coupled plasma-mass spectrometry (ICP-
27
28 MS) when operated in a time-resolved mode with very short signal integration periods, called
29
30 dwell times. This configuration has already demonstrated encouraging results for analysis of
31
32 nanomaterials and is often referred to as single-particle ICP-MS (spICP-MS).¹⁹⁻²¹ The method
33
34 provides “particle by particle” measurements that include information about particle number
35
36 concentration, particle size, and size distribution.²¹ Each particle that enters the ICP plasma
37
38 forms an ion cloud that results in an isotope count registered by the MS during a single dwell
39
40 time measurement.^{22, 23} Although most spICP-MS applications to date have focused on the
41
42 characterization and direct quantification of nanoparticles themselves,^{24, 25} the capacity for
43
44 ultralow detection of the particle concentration also makes spICP-MS a promising tool for
45
46 ultrasensitive bioassays.^{26, 27} Zhang *et al.* developed a multiple DNA assay using different
47
48 isotopes of nanoparticles as the output signal. The nanoparticles were first captured by the
49
50
51
52
53
54
55
56
57
58
59
60

1
2
3 heterogeneous sandwich structure and then melted and washout into the ICP-MS. The
4
5 nanoparticle concentration quantified by spICP-MS was proportional to the concentration of the
6
7 target.²⁸
8
9

10 Considering the characteristics of ultrasensitive detection and methods with an ultralow detection
11
12 limits (sub-picomolar),¹⁴ the detection of ultralow concentrations of biomarkers, such as
13
14 bloodborne viruses, circulating tumor cells, and circulating nucleic acids,²⁹ might be met by
15
16 using spICP-MS measurements as the signaling system. Based on this hypothesis, we developed
17
18 an ultrasensitive yet versatile graphene platform for detecting and quantifying the model
19
20 biomarker thrombin using gold nanoparticles (AuNPs) and spICP-MS methods. Thrombin is a
21
22 kind of serine protease that plays a crucial role in blood coagulation and is a biomarker for
23
24 venous thrombosis, thrombophilia, abnormal coagulation, and hundreds of other disease
25
26 states.^{10, 30, 31} We fabricated a sensing platform based on GO/DNA recognition and spICP-MS
27
28 detection of AuNPs coupled to that recognition. An ultralow detection limit of 4.5 fM was
29
30 archived by the combination of excellent recognition ability of GO for ssDNA and single
31
32 nanoparticle of spICP-MS. Moreover, the diversity and ready availability of ssDNA sequences
33
34 that can be bound to AuNPs make then an excellent building block for various targets because
35
36 they can work as an aptamer or as a complementary sequence.^{32, 33} Hence, our combined sensing
37
38 platform and spICP-MS method has potential as a broad-spectrum bioassay for ultrasensitive
39
40 detection of biomarkers in clinical diagnostics.
41
42
43
44
45

46 47 **2. Experimental Section**

48 49 **2.1. Materials and reagents**

50
51 Gold nanoparticles (20 nm) were purchased from Cytodiagnostics Inc (Burlington, Canada).
52
53 Gold standard solution was purchased from Inorganic Ventures (Christiansburg, VA). High
54
55
56
57
58
59
60

1
2
3 purity liquid argon was used as the plasma gas and the nebulizer gas for all ICP-MS
4
5 measurements. In the conventional ICP-MS measurements, an ultra-high purity helium gas was
6
7 used to remove undesirable molecule ions in the kinetic energy discrimination (KED) mode. (11-
8
9 mercaptoundecyl) hexa (ethylene glycol) (TOEG6), Tris(2-carboxyethyl)phosphine
10
11 hydrochloride (TCEP), sodium chloride, magnesium chloride, sodium phosphate monobasic,
12
13 sodium phosphate dibasic, sodium citrate tribasic dihydrate, bovine serum albumin (BSA),
14
15 thrombin from human plasma and 0.22 μm filter membranes were purchased from Sigma-
16
17 Aldrich (St. Louis, MO). Immunoglobulin G (IgG) was purchased from Santa Cruz
18
19 Biotechnology (Dallas, TX). Fetal bovine serum (FBS) was purchased from VWR (Radnor, PA).
20
21 Single layer graphene oxide was purchased from ACS Material (Pasadena, CA). The deionized
22
23 (DI) water (18.2 $\text{M}\Omega\cdot\text{cm}$) was produced from a Millipore water purification system. All DNA
24
25 sequences were synthesized by Integrated DNA Technology (Coralville, IA). The sequences³⁴ of
26
27 DNA used were as follows:
28
29

30
31
32 m29: 5'-HS-(CH₂)₆-TTTTTAGTCCGTGGTAGGGCAGGTTGGGGTGACT

33
34
35 m29-F: 5'-HS-(CH₂)₆-TTTTTAGTCCGTGGTAGGGCAGGTTGGGGTGACT-Alex750-3'

36 37 38 **2.2. Instruments**

39
40 UV-Vis absorption measurements were performed on a PerkinElmer Lambda 1050 UV/Vis/NIR
41
42 spectrometer (PerkinElmer, Santa Clara, CA), equipped with a Peltier temperature control
43
44 accessory. Zeta potential of nanomaterials was measured using Zetasizer nano (Malvern
45
46 Panalytical, UK). Fluorescence spectra were obtained with an RF-6000 spectrophotometer
47
48 (Shimadzu, Japan). Transmission electron microscopy (TEM) images of GO and AuNPs were
49
50 taken using a Hitachi 7500 transmission electron microscope (Hitachi, Japan). All ICP-MS
51
52 measurements were carried out using a Thermo Scientific iCAP Qc ICP-MS (Bremen, Germany)
53
54
55
56
57
58
59
60

1
2
3 coupled with a 4-channel 12-roller peristaltic pump, nickel sample and skimmer cones, a
4
5 Teledyne CETAC ASX560 autosampler (Omaha, NE), a microflow perfluoroalkoxy nebulizer
6
7 (Thermo Scientific) and a Peltier-cooled quartz cyclonic spray chamber. To monitor the ICP-MS
8
9 instrument, the THERMO-4AREV (Thermo Scientific) standard was run daily for maximum
10
11 ^{59}Co , ^{238}U and minimum $^{140}\text{Ce}^{16}\text{O}/^{140}\text{Ce}$ signal. The ICP-MS measurements of AuNPs were
12
13 controlled by the QtegraTM software (version 2.8.2944.202). The instrument operating
14
15 parameters used for the single particle and conventional ICP-MS measurements are listed in
16
17 Table S1 (Supporting Information).
18
19
20

21 **2.3. Preparation of ssDNA modified AuNPs**

22
23 Thiol-functionalized ssDNA (SH-ssDNA) (100 μL of 200.0 μM) was reduced in the 100 μL of
24
25 TCEP (20.0 mM), and then was incubated for 2 h at room temperature. The amount of ssDNA
26
27 was quantified with UV-Vis spectrometry. The modification of AuNPs with ssDNA was
28
29 performed according to the literature with a slight change.³⁵ Briefly, the reduced SH-ssDNA (10
30
31 μL of 100.0 μM) was mixed with 1.0 mL of 1 OD 20-nm-diameter AuNPs under vortexing for 1
32
33 min and was retained in the container for 10 min at room temperature. Afterward, a 100 μL
34
35 aliquot of citrate-HCl buffer (100 mM, pH 4.3) was added to adjust the pH of the solution and
36
37 the mixture was incubated for 30 min, followed by a 50 μL addition of 300.0 μM TOEG6. After
38
39 an additional 10 min of static incubation, the solution was centrifuged at 6,500 $\times g$ for 30 min.
40
41 The precipitates were collected and washed twice with DI water. The final pellet was re-
42
43 dispersed in 1.0 mL of DI water and stored at 4 $^{\circ}\text{C}$ for further use.
44
45
46
47
48

49 **2.4. Adsorption of ssDNA to GO**

50
51 A 50 μL aliquot of 5×10^{11} particle/mL AuNPs-ssDNA and 50 μL of 400.0 $\mu\text{g}/\text{mL}$ of GO were
52
53 incubated in 1.0 mL of PBS buffer (10 mM with 0.5 mM MgCl_2 , pH 7.4) at room temperature
54
55
56
57
58
59
60

1
2
3 for 30 min with regular shaking. Then the solution was vacuum filtered through a 0.22 μm pore
4 membrane. After washing twice with water and once with PBS buffer, the maroon-colored
5 GO/AuNPs composites distributed on the membrane surface were re-dispersed in 2 mL of PBS
6
7
8
9
10 buffer by using an ultrasonic water bath.

11 **2.5. Analysis of thrombin by GO/AuNPs composites using spICP-MS**

12
13
14 A 50 μL aliquot of thrombin solution with varied concentration was incubated with 50 μL of
15 prepared GO/AuNPs composites in a total of 500 μL of PBS buffer (10 mM with 0.5 mM
16
17
18
19
20
21
22
23
24
25
26
27
28
29
30
31
32
33
34
35
36
37
38
39
40
41
42
43
44
45
46
47
48
49
50
51
52
53
54
55
56
57
58
59
60
MgCl₂, pH 7.4) at 37 °C with regular shaking. After 1 h of incubation, the solution was removed
by syringe and filtered using a 0.22 μm membrane. After 10 min of ultrasonic agitation in a
water bath, the filtrate analyzed by spICP-MS.

3. Results and discussion

3.1. Design and function of the bioassay platform

The graphene-based sensing platform was based on spICP-MS direct-counting of AuNPs that
desorb from a designed GO/AuNPs composite. Desorption is caused by a reaction between the
target biomolecule and the ssDNA ligands (aptamer) modified on the surface of the AuNPs. The
sequential design of this platform is illustrated in Scheme 1. First, a thrombin-selective aptamer
(ssDNA sequence with strong affinity to thrombin) is covalently immobilized on the surface of
20 nm citrate stabilized AuNPs through the formation of an Au-S bond. After incubation with a
GO sheet, the aptamer modified AuNPs are adsorbed on the surface of GO due to the strong π - π
stacking interaction between the ring structures of ssDNA base and the GO sheet, thereby
forming the GO/AuNPs composite (Scheme 1A). After thoroughly washing to remove any free
AuNPs, the target biomolecule, thrombin, is introduced to the platform. In the presence of
thrombin, aptamer on the AuNPs complexes with the thrombin molecule and changes the

1
2
3 aptamer structure (Scheme 1B). This conformational change breaks the interaction between the
4
5 aptamer and the GO, causing the associated AuNPs-aptamer to desorb from the GO surface.
6
7 Before introducing the solution into the spICP-MS, it is filtered to remove the AuNPs still
8
9 adsorbed to GO. In this way, only the desorbed, thrombin-complexed AuNPs are injected into
10
11 the ICP-MS (Scheme 1C) and there should be no aptamer-modified AuNPs desorbed in the
12
13 absence of thrombin (Scheme 1D). Individual AuNPs are detected in the single-particle analysis
14
15 mode as a measured count of $^{197}\text{Au}^+$ above a certain background threshold. The number of
16
17 detected AuNPs are directly related to the number of AuNPs desorbed from GO by thrombin-
18
19 aptamer complexation and also to the thrombin concentration. Because the spICP-MS method
20
21 can easily detect even small number (<100) of AuNPs per mL of solution, this assay should be
22
23 able to achieve ultralow detection limits for thrombin or other potential biomarkers.
24
25
26
27

28 **3.2. Formation of GO/AuNPs composites**

29
30 Two signaling modes have been used for the graphene/DNA based fluorescence bioassays. Both
31
32 modes depend on the sequence of ssDNA adsorbed to the GO.^{7, 36} The “turn off” mode, also
33
34 termed the post-adsorb strategy, requires incubation of the target molecule with dye modified
35
36 ssDNA, followed by addition of GO to cause fluorescence quenching after the unbound ssDNA
37
38 is adsorbed to the GO surface. The “turn on” mode, also termed the pre-adsorb strategy, requires
39
40 initial adsorption of the dye modified ssDNA reagent to the GO surface in order to start with the
41
42 fluorescence quenched. Subsequent addition of target molecules causes desorption of dye
43
44 molecules from the GO platform due to the interaction with ssDNA, resulting in fluorescence
45
46 recovery. Because a higher signal to noise ratio is inherent to the “turn on” or pre-adsorb
47
48 strategy, the developed assay used GO/AuNPs composites that were preassembled before
49
50 incubation with thrombin.
51
52
53
54
55
56
57
58
59
60

1
2
3 Unlike adsorption between dye-modified ssDNA and GO, unmodified AuNPs were easily
4 adsorbed to GO in high ionic-strength buffers, although both were negatively charged (Figure
5 S1, Supporting Information). Strong van der Waals forces play a significant role in aggregation
6 of AuNPs and GO through the screening of charge repulsions at high salt concentrations.³⁷
7
8 Accordingly, a moderate salt concentration is required to favor the adsorption of ssDNA to GO
9 and avoid nonspecific adsorption of AuNPs to GO. To determine the most favorable ionic
10 strength, the salt concentration was optimized. As shown in Figure 1, the amount of AuNPs
11 measured in the filtrate after incubating with GO in a PB buffer was found to vary with different
12 concentrations of Mg²⁺ or Na⁺. The difference was quantified by measuring the UV-Vis
13 absorbance peak at 520 nm for 20 nm AuNPs. For 0.5 mM MgCl₂ (Figure 1A), around 100% of
14 the AuNP-TOEG6 (red circle, control group without ssDNA modification) was recovered in the
15 filtrate after incubating with GO, indicated that there was no nonspecific binding between the
16 AuNPs and GO. When the MgCl₂ concentration was higher than 1.0 mM, less than 70 % of the
17 AuNPs were recovered in the filtrate. The unrecovered AuNPs were non-specifically bound to
18 the GO surface, so these conditions should be avoided. For all MgCl₂ concentrations, the
19 aptamer modified AuNPs (black squares) were easily adsorbed to the GO surface and retained.
20 Moreover, there was no aptamer modified AuNPs left in the filtrate after incubating with GO in
21 the buffer solution with MgCl₂ concentration higher than 2.0 mM. Although the adsorption
22 efficiency was not 100 % under 0.5 mM MgCl₂ concentration, this concentration was optimal
23 considering the nonspecific adsorption to the AuNPs without ssDNA. The same situation was
24 also observed when using NaCl (Figure 1B). However, the nonspecific adsorption still existed
25 even when the concentration of NaCl was only 10.0 mM, which was much lower than the
26
27
28
29
30
31
32
33
34
35
36
37
38
39
40
41
42
43
44
45
46
47
48
49
50
51
52
53
54
55
56
57
58
59
60

1
2
3 required concentration of Na^+ for the interaction between ssDNA and GO.³⁸ Therefore, PB
4 buffer with 0.5 mM MgCl_2 was chosen for the incubation of aptamer modified AuNPs and GO.
5
6 Formation of the composite was confirmed visually by 0.22 μm filtration at four stages of
7
8 GO/AuNPs synthesis (Figure 2). GO was retained on the filter membrane surface (brown color)
9
10 because of its larger average size (>500 nm) than the membrane pore size (0.22 μm , Figure 2A).
11
12 The AuNPs-aptamer, which was only 20 nm in diameter, passed the membrane easily and no
13
14 evidence of the residual AuNPs was seen on the membrane surface (Figure 2B). When the
15
16 GO/AuNPs composites formed by incubation of GO and AuNPs-aptamer, the residue on the
17
18 membrane was a reddish brown color, resulting from the color of AuNPs on GO (Figure 2C).
19
20 The residue of the GO and AuNPs-TOEG6 (Figure 2D) was the same as the pure GO (Figure
21
22 2A), indicating no AuNPs nonspecifically adsorbed onto the GO. Formation of the GO/AuNPs
23
24 composite was further confirmed by TEM images (Figure S2C, Supporting Information). the GO
25
26 was present in a classic one-layer sheet structure with the size larger than 500 nm. The 20 nm
27
28 AuNPs (dark spots) were evenly distributed on the GO surface. No free AuNPs existed in the
29
30 area without GO.
31
32
33
34
35
36

37 **3.3. Validation of spICP-MS for ultrasensitive detection**

38
39 The feasibility of ultrasensitive detection of AuNPs by spICP-MS was first verified. As shown in
40
41 Scheme 1, the measured signal of the method is the number of desorbed AuNPs, which is
42
43 proportional to the concentration of the target molecule. Solutions containing different number
44
45 concentrations of standard AuNPs were tested using the spICP-MS. As shown in Figure 3, the
46
47 number of detected AuNPs (i.e., measurements significantly greater than background) within 30
48
49 s systematically increased when the AuNP number concentration increased. The NP detection
50
51 criterion applied in all measurements was signal (in counts) greater than five-times the baseline
52
53
54
55
56
57
58
59
60

1
2
3 noise level. This noise level was 1 count, so a NP was detected if the signal intensity was higher
4 than 5 counts. There were no detected NPs in the blank solution without AuNPs (Figure 3A). By
5 increasing the particle number concentration from 100 to 100,000 particles/mL, the number of
6 NPs detected during the 180 s acquisition period increased from 2 to ~800 (Figure 3B-G). The
7 relationship between the number of detected NPs and the particle number concentration was
8 calibrated under conditions of 0.20 $\mu\text{L}/\text{min}$ flow rate and 6.45 % transport efficiency. The results
9 showed an excellent linear fit at a low concentration range (0-10,000 particles/mL, Figure 3H
10 inset). Hence, the number concentration of AuNPs in the solution could be absolutely quantified
11 by using this calibration and the volume of the sample measured during the acquisition period.
12 The number of AuNPs detected at high concentrations was lower than the expectation from the
13 linear part of the calibration curve (Figure 3H). This was probably by the greater likelihood of
14 two AuNPs entering the plasma within one dwell time.
15
16

17
18
19 To demonstrate the greater capacity of spICP-MS for ultrasensitive assays using AuNPs, we
20 compared the spICP-MS measurements of AuNP solutions with conventional ICP-MS
21 measurements. For the later, an average $^{197}\text{Au}^+$ signal for many AuNPs (rather than a discreet
22 signal from one AuNP) is measured because repeated sampling (10 sweeps) and a much a longer
23 integration period (50 ms dwell time) is used. The results are listed in Table S2 (Supporting
24 Information). The Au detection limit using conventional ICP-MS was 0.005 ppb, which was
25 calibrated using gold standard solutions. There were no Au detected by conventional ICP-MS
26 when the particle number concentration was lower than 10^6 particles/mL. In contrast, a solution
27 of 100 particle/mL could be easily determined using the single particle mode with only a 3 min
28 collection time. Note that the detection limit of the spICP-MS method could be even lower if the
29 collection time was increased.²² Moreover, the theoretical number of detected NPs calculated
30
31
32
33
34
35
36
37
38
39
40
41
42
43
44
45
46
47
48
49
50
51
52
53
54
55
56
57
58
59
60

1
2
3 based on the literature²² was close to the experimental data, demonstrating the reliability of the
4 method. These data demonstrated that even if only a few hundred AuNPs desorbed from GO
5 induced by a thrombin sample, they could be easily quantified by spICP-MS. Assuming each
6 thrombin molecule of the 1 mL sample would desorb one AuNP and that each AuNP would be
7 detected, this analytical performance would correspond to a thrombin concentration of less than
8 1×10^{-18} M.
9

17 **3.4. Optimizations**

19 Unlike the dye-based signaling molecules used in fluorescence bioassays, there are numerous
20 positions on AuNPs that can be bound with ssDNA when used for signaling in spICP-MS
21 bioassays. The high loading capacity of ssDNA on AuNPs can strengthen the interaction
22 between the modified AuNPs and GO. However, heavily modified AuNPs can become too hard
23 to desorb in the presence of target. Hence, the ssDNA density on the AuNPs, which would affect
24 the desorption efficiency of ssDNA in the thrombin, was optimized prior to the detection.
25 TOEG6, a protein-repellent alkanethiol, was used to stabilize the AuNPs by passivating the
26 particle surface during the ssDNA immobilization. The amount of ssDNA on the AuNPs surface
27 was tuned by changing the ratio of ssDNA to TOEG6.³⁵ The exact amount of ssDNA was
28 quantified by measuring the supernatant fluorescence of Alex-750 appended to the free end of
29 the thrombin aptamer. The ssDNA density on AuNPs at different concentrations of TOEG6 is
30 summarized in Table S3 (Supporting Information). The higher the TOEG6 concentration, the
31 lower ssDNA density on the AuNPs. Finally, an average of one ssDNA per particle was obtained
32 when the TOEG6 concentration increased to 15 μ M, which was 60-times higher than the ssDNA
33 concentration. After obtaining aptamer-modified AuNPs with different numbers of immobilized
34 ssDNA, the assay was optimized based on the number of AuNPs detected by spICP-MS. As
35
36
37
38
39
40
41
42
43
44
45
46
47
48
49
50
51
52
53
54
55
56
57
58
59
60

1
2
3 shown in Figure 4A, the number of detected AuNPs increased with decreasing number of
4 immobilized ssDNA, demonstrating that AuNPs with less immobilized aptamer would more
5 easily desorb from the GO surface under the same concentration of thrombin. To achieve the best
6 result, AuNPs with an average of one ssDNA per particle was chosen as the optimum aptamer
7 modified AuNP reagent. Some of the AuNPs might contain no ssDNA; however, this would not
8 affect the assay because those AuNPs without ssDNA could be washed out by passing the filter
9 membrane before introducing to the target molecules. The results in Figure 2 support that these
10 AuNPs with TOEG6 had little attraction with the GO.
11
12
13
14
15
16
17
18
19
20

21 To guarantee that the reaction of thrombin with aptamer reached equilibrium before spICP-MS
22 analysis, the incubation time of thrombin and GO/AuNPs composites was investigated. As
23 shown in Figure 4B, the number of detected NPs increased quickly with incubation time during
24 the first 30 min but reached a plateau at 60 min. There was no further change even when the
25 incubation time was extended to 2 h. As a result, the incubation time of 60 min was determined
26 as the optimal reaction time for the assay method.
27
28
29
30
31
32
33
34

35 **3.5. Sensitivity to thrombin concentration**

36 The assay was applied to thrombin determination using the spICP-MS under the optimized
37 conditions. As shown in Figure 6, the number of detected AuNPs systematically increased within
38 the 30 s collection time as the thrombin concentration increased from 1.0 fM to 10.0 nM. There
39 were also a few detected AuNPs without adding thrombin in the blank (Figure 5A). The
40 concentration of residual AuNPs in the blank was as high as $(40 \pm 6) \times 10^3$ particle/mL after
41 washing steps. Moreover, there was no difference between the blank sample and the sample with
42 0.1 fM of the thrombin, which established a concentration below the detection limit of the
43 method (Figure 5B). With the 1.0 fM of thrombin sample, there was a noticeable increase in
44
45
46
47
48
49
50
51
52
53
54
55
56
57
58
59
60

1
2
3 detected AuNPs compared with blank, although the distinction was only slight (Figure 5C).
4
5 When the concentration of thrombin was higher than 10.0 fM, the number of detected AuNPs
6
7 increased dramatically (Figure 5D-J).
8
9

10 The quantitative relationship between the concentration of thrombin and the concentration of
11
12 desorbed AuNPs is demonstrated in Figure 6. Here, N_0 is the number of detected AuNPs in the
13
14 blank as control and N is the number of detected AuNPs at different thrombin concentrations.
15
16 This assay showed a broad dynamic range from 1.0 fM to 10.0 nM. It also showed a logarithmic
17
18 relationship with the thrombin concentration from 10.0 fM to 100.0 pM (Figure 6 inset) with a
19
20 correlation coefficient (R^2) of 0.9997. The limit of detection was estimated to be 4.5 fM by the
21
22 3σ rule, which was around five orders of magnitude lower than the similar graphene based
23
24 fluorescence platform.^{6, 10}
25
26
27

28 **3.6. Selectivity**

29
30 The specificity of the developed sensor was evaluated by testing other protein components in a
31
32 serum sample. As shown in Figure 7, the desorbed AuNPs detected by reacting with BSA, IgG,
33
34 and FBS respectively at a concentration of 1.0 μ M (\sim 0.1 g protein/L for FBS) were less than
35
36 10% of that caused by thrombin at a concentration of 10.0 pM. This result strongly demonstrated
37
38 that the method could be used for both selective and sensitive detection of the target
39
40 biomolecules. Moreover, based on the recovery measurement for FBS sample spiked with 10 pM
41
42 of thrombin (recovery: $117 \pm 13\%$), the fact that the sample of thrombin in FBS showed the same
43
44 signal level compared to the pure thrombin showed that the method was not significantly
45
46 influenced by interferences and indicated its great potential for applications with complex sample
47
48 interferences.
49
50
51
52

53 **4. Conclusions**

54
55
56
57
58
59
60

1
2
3 An effective and versatile GO/AuNPs platform for ultrasensitive detection of target biomarkers
4 using spICP-MS technology was developed. In this case, thrombin was used as a model target
5
6 biomarker and could be detected at as low concentration as 4.5 fM. Compare with similar
7
8 fluorescence-based platforms this detection limit was lower by five orders of magnitude, making
9
10 this method comparable to other ultrasensitive methods for thrombin.^{39, 40} It is also noteworthy
11
12 that this detection limit could be further reduced by removing the free AuNPs in the GO/AuNPs
13
14 composites or coupling an amplification strategy. Because of the excellent specificity of the
15
16 aptamer,³² this platform also showed high selectivity. Moreover, the type nanoparticles used as a
17
18 metal isotope signal for spICP-MS could be varied, making it possible for simultaneous detection
19
20 of multiple biomarkers if a time-of-flight mass spectrometer was employed. Finally, the
21
22 method's minimal interference from the matrix makes it suitable for applications in clinical
23
24 diagnostics.
25
26
27
28
29
30

31 **Conflicts of interest**

32
33
34 There are no conflicts to declare.
35

36 **Acknowledgments**

37
38
39 This work was supported by the NSF grant CHE 1709160 (J.X.Z.) UND Applied Research to
40 Address the State's Critical Needs Initiative program (X.W.) and the NIH grant
41 5P20GM103442-18 (D.T.P). The authors acknowledge the use of the Edward C. Carlson
42 Imaging and Image Analysis Core Facility which is supported in part by NIH grant
43 1P20GM113123 and P20GM103442 and also acknowledge use of the North Dakota INBRE
44 Metal Analysis Core Facility, which is supported in part by NIH grant 5P20GM103442-18.
45
46

47 **Supporting Information**

48
49 Instrument parameters of ICP-MS, Zeta potential, TEM characterization of nanomaterials.
50
51 SsDNA modification density on AuNPs, Comparison of AuNPs quantification by two models of
52
53 ICP-MS.
54
55
56
57
58
59
60

1
2
3 **Co-Corresponding Authors**
4

5
6 julia.zhao@und.edu (J.X. Zhao)
7

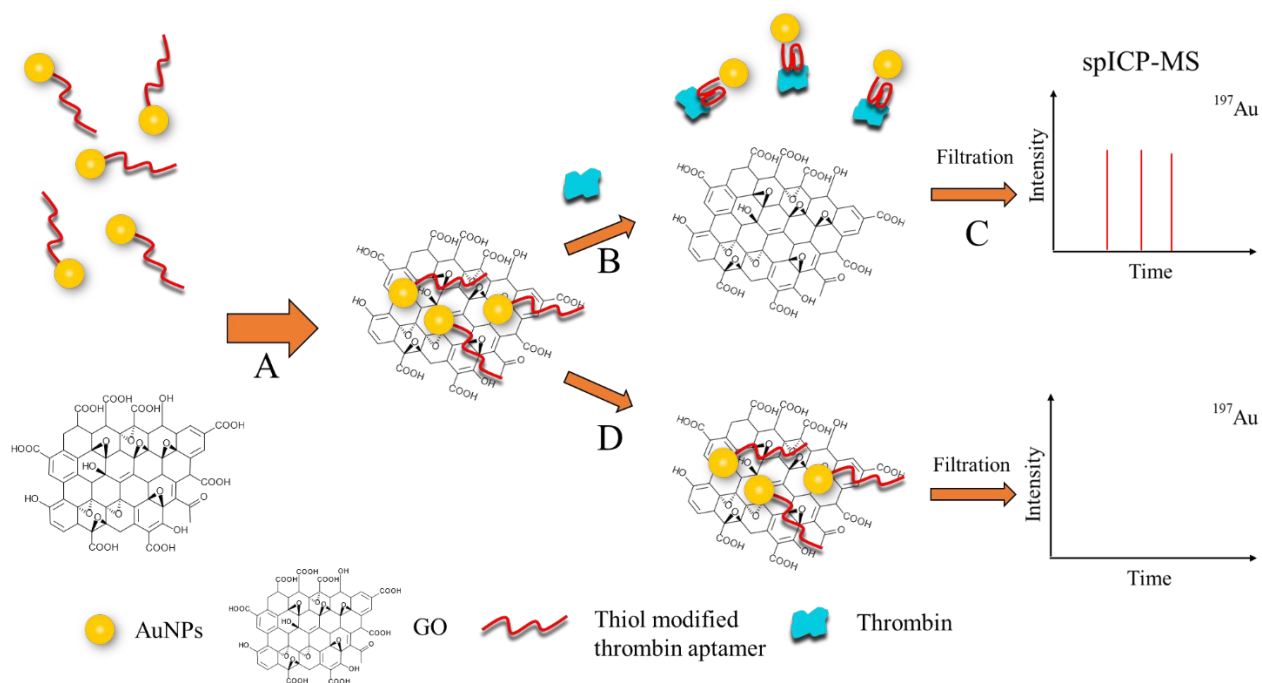
8 david.pierce@und.edu (D.T. Pierce)
9
10
11
12
13
14
15
16
17
18
19
20
21
22
23
24
25
26
27
28
29
30
31
32
33
34
35
36
37
38
39
40
41
42
43
44
45
46
47
48
49
50
51
52
53
54
55
56
57
58
59
60

Reference

1. X. Wu, F. Mu, Y. Wang and H. Zhao, *Molecules* 2018, **23**, 2050.
2. Y. Liu, X. Dong and P. Chen, *Chem. Soc. Rev.* 2012, **41**, 2283-2307.
3. X. Huang, Z. Yin, S. Wu, X. Qi, Q. He, Q. Zhang, Q. Yan, F. Boey and H. Zhang, *Small* 2011, **7**, 1876-1902.
4. J. Kim, L. J. Cote and J. Huang, *Acc. Chem. Res.* 2012, **45**, 1356-1364.
5. Z. Liu, B. Liu, J. Ding and J. Liu, *Anal. Bioanal. Chem.* 2014, **406**, 6885-6902.
6. C. H. Lu, H. H. Yang, C. L. Zhu, X. Chen and G. N. Chen, *Angew. Chem. Int. Ed. Engl.* 2009, **48**, 4785-4787.
7. P. Alonso-Cristobal, P. Vilela, A. El-Sagheer, E. Lopez-Cabarcos, T. Brown, O. L. Muskens, J. Rubio-Retama and A. G. Kanaras, *ACS Appl. Mater. Interfaces* 2015, **7**, 12422-12429.
8. M. Li, X. Zhou, S. Guo and N. Wu, *Biosens. Bioelectron.* 2013, **43**, 69-74.
9. Y. He, Y. Lin, H. Tang and D. Pang, *Nanoscale* 2012, **4**, 2054-2059.
10. H. Chang, L. Tang, Y. Wang, J. Jiang and J. Li, *Anal. Chem.* 2010, **82**, 2341-2346.
11. M. Zhang, B. C. Yin, W. Tan and B. C. Ye, *Biosens. Bioelectron.* 2011, **26**, 3260-3265.
12. Y. Wang, Z. Li, J. Wang, J. Li and Y. Lin, *Trends Biotechnol.* 2011, **29**, 205-212.
13. J. Pena-Bahamonde, H. N. Nguyen, S. K. Fanourakis and D. F. Rodrigues, *J. Nanobiotech.* 2018, **16**, 75.
14. Y. Wu, R. D. Tilley and J. J. Gooding, *J. Am. Chem. Soc.* 2018, **141**, 1162-1170.
15. Y. Zhao, F. Chen, Q. Li, L. Wang and C. Fan, *Chem. Rev.* 2015, **115**, 12491-12545.
16. E. Vermisoglou, D. Panáček, K. Jayaramulu, M. Pykal, I. Frébort, M. Kolář, M. Hajdúch, R. Zbořil and M. Otyepka, *Biosens. Bioelectron.* 2020, **166**, 112436.
17. J. Anna, J. Aleksandra, K. Mateusz, B. Sylwia and P. Barbara, *Curr. Med. Chem.* 2019, **26**, 6878-6895.
18. W. Wang, H. Su, Y. Wu, T. Zhou and T. Li, *J. Electrochem. Soc.* 2019, **166**, B505-B520.

19. M. D. Montano, J. W. Olesik, A. G. Barber, K. Challis and J. F. Ranville, *Anal. Bioanal. Chem.* 2016, **408**, 5053-5074.
20. C. Degueldre and P. Y. Favarger, *Colloids Surf. A Physicochem. Eng. Asp.* 2003, **217**, 137-142.
21. F. Laborda, E. Bolea and J. Jimenez-Lamana, *Anal. Chem.* 2014, **86**, 2270-2278.
22. F. Laborda, J. Jiménez-Lamana, E. Bolea and J. R. Castillo, *J. Anal. At. Spectrom.* 2013, **28**, 1220-1232.
23. F. H. Lin, S. I. Miyashita, K. Inagaki, Y.H. Liu and I. H. Hsu, *J. Anal. At. Spectrom.* 2019, **34**, 401-406.
24. A. R. Montoro Bustos, E. J. Petersen, A. Possolo and M. R. Winchester, *Anal. Chem.* 2015, **87**, 8809-8817.
25. R. Peters, Z. Herrera-Rivera, A. Undas, M. van der Lee, H. Marvin, H. Bouwmeester and S. Weigel, *J. Anal. At. Spectrom.* 2015, **30**, 1274-1285.
26. J. Hu, D. Deng, R. Liu and Y. Lv, *J. Anal. At. Spectrom.* 2018, **33**, 57-67.
27. G. Han, Z. Xing, Y. Dong, S. Zhang and X. Zhang, *Angew. Chem. Int. Ed. Engl.* 2011, **50**, 3462-3465.
28. S. Zhang, G. Han, Z. Xing, S. Zhang and X. Zhang, *Anal. Chem.* 2014, **86**, 3541-3547.
29. S. O. Kelley, *ACS Sens.* 2017, **2**, 193-197.
30. A. Bini, M. Minunni, S. Tombelli, S. Centi and M. Mascini, *Anal. Chem.* 2007, **79**, 3016-3019.
31. R. C. Becker, *J. Thromb. Thrombolysis* 2005, **19**, 71-75.
32. M. Ilgu and M. Nilsen-Hamilton, *Analyst*, 2016, **141**, 1551-1568.
33. L. Yan, J. Zhou, Y. Zheng, A. S. Gamson, B. T. Roembke, S. Nakayama and H. O. Sintim, *Mol. Biosyst.* 2014, **10**, 970-1003.
34. Y. Liu, N. Liu, X. Ma, X. Li, J. Ma, Y. Li, Z. Zhou and Z. Gao, *Analyst*, 2015, **140**, 2762-2770.
35. J. Deka, R. Mech, L. Ianeselli, H. Amenitsch, F. Cacho-Nerin, P. Parisse and L. Casalis, *ACS Appl. Mater. Interfaces* 2015, **7**, 7033-7040.
36. J. Lee, J. Kim, S. Kim and D. H. Min, *Adv. Drug Deliv. Rev.* 2016, **105**, 275-287.
37. J. Liu, *Phys. Chem. Chem. Phys.* 2012, **14**, 10485-10496.

- 1
2
3
4 38. M. Wu, R. Kempaiah, P. J. Huang, V. Maheshwari and J. Liu, *Langmuir*, 2011,
5 27, 2731-2738.
6
7 39. Y. Zhang, J. Xia, F. Zhang, Z. Wang and Q. Liu, *Sens. Actuators B Chem.* 2018,
8 267, 412-418.
9
10 40. C. Wang, Y. Qian, Y. Zhang, S. Meng, S. Wang, Y. Li and F. Gao, *Sens.*
11 *Actuators B Chem.* 2017, 238, 434-440.
12
13
14
15
16
17
18
19
20
21
22
23
24
25
26
27
28
29
30
31
32
33
34
35
36
37
38
39
40
41
42
43
44
45
46
47
48
49
50
51
52
53
54
55
56
57
58
59
60



Scheme 1. Schematic illustration of thrombin detection using aptamer modified AuNPs by spICP-MS. A, thrombin aptamer modified AuNPs incubated with GO; B, thrombin molecule as target incubated with GO/AuNPs composites; C, desorbed AuNPs were separated and introduced into spICP-MS; D, no thrombin molecule added as control.

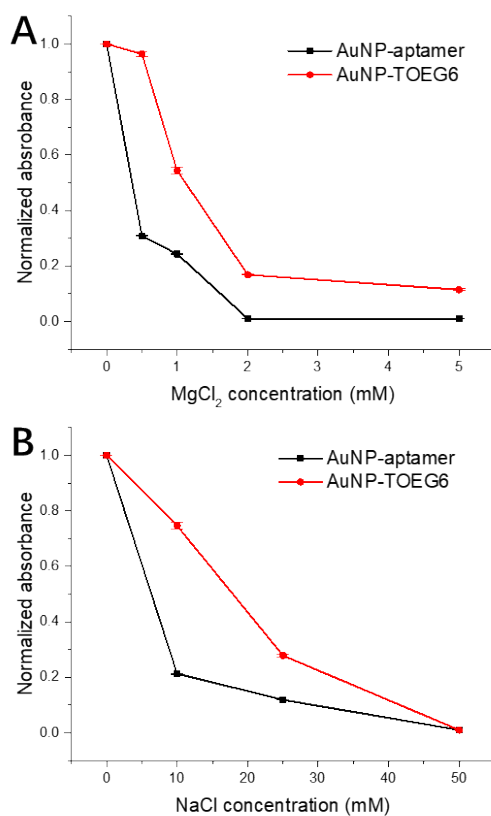


Figure 1. UV-Vis absorption of AuNPs at 520 nm with different concentration of MgCl₂ (A) or NaCl (B). The AuNPs were in the filtrate after incubation with GO in a PB buffer (10.0 mM, pH 7.4)

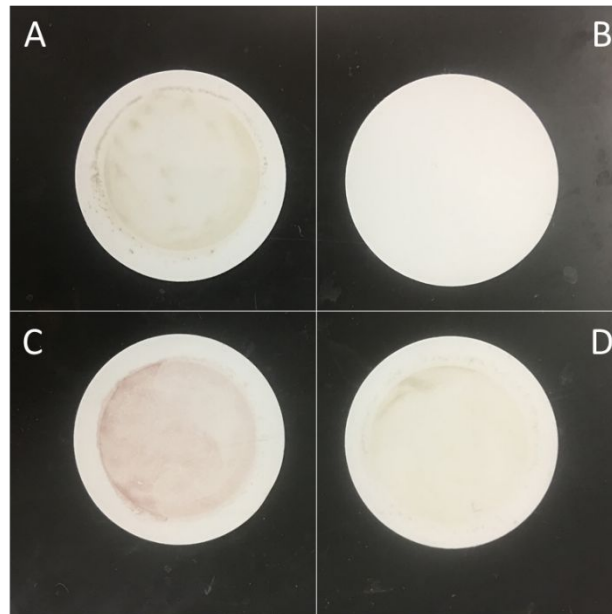


Figure 2. Photos of GO/AuNPs collected on the filter membrane surface. A, GO only; B, AuNP-aptamer only; C, GO and AuNP-aptamer; D, GO and AuNP-TOEG6. Incubated in 1.0 mL of 10.0 mM PB buffer with 0.5 mM MgCl_2 (pH 7.4) for 10 min at room temperature. The GO concentration: 20 $\mu\text{g}/\text{mL}$; AuNPs concentration: 10^{10} nanoparticles/mL.

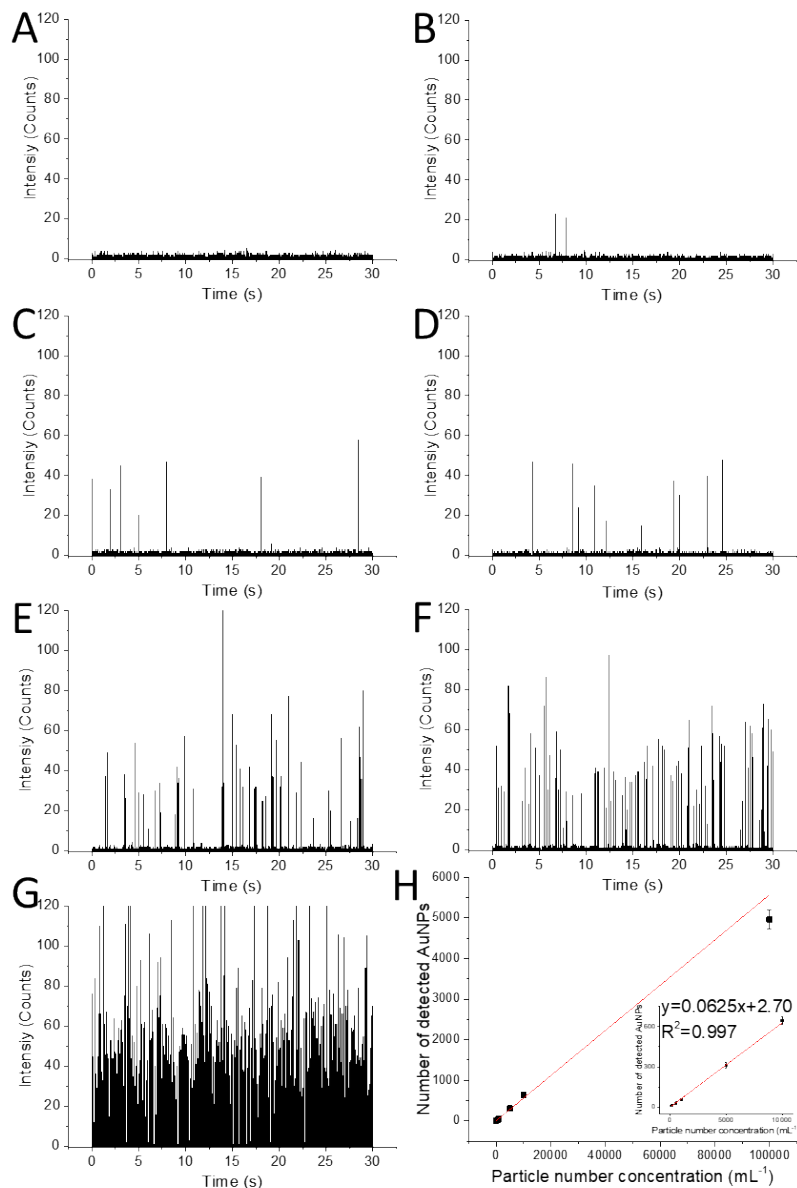


Figure 3. spICP-MS spectra of AuNPs in different particle number concentrations. A-G: 0, 100, 500, 1,000, 5,000, 10,000, and 100,000 particles/mL. (¹⁹⁷Au, dwell time: 5 ms). H. Relationship between the number of detected AuNPs and the particle number concentration from 0 to 100,000 particles/mL within 180 s collection time. Inset: Calibration curve of the number of detected AuNPs and the particle number concentration from 0 to 10,000 particles/mL.

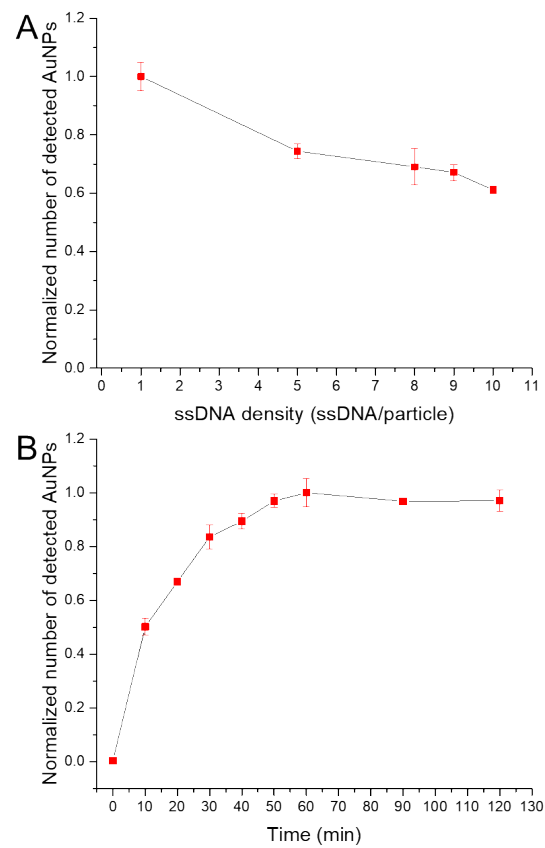


Figure 4. The optimizations of aptamer density on AuNPs (A), and incubation time (B).
Thrombin concentration: 10 pM. GO/AuNPs composites concentration: 1 $\mu\text{g}/\text{mL}$ (GO mass based) Incubation in PBS buffer (10 mM with 0.5 mM MgCl_2 , pH 7.4).

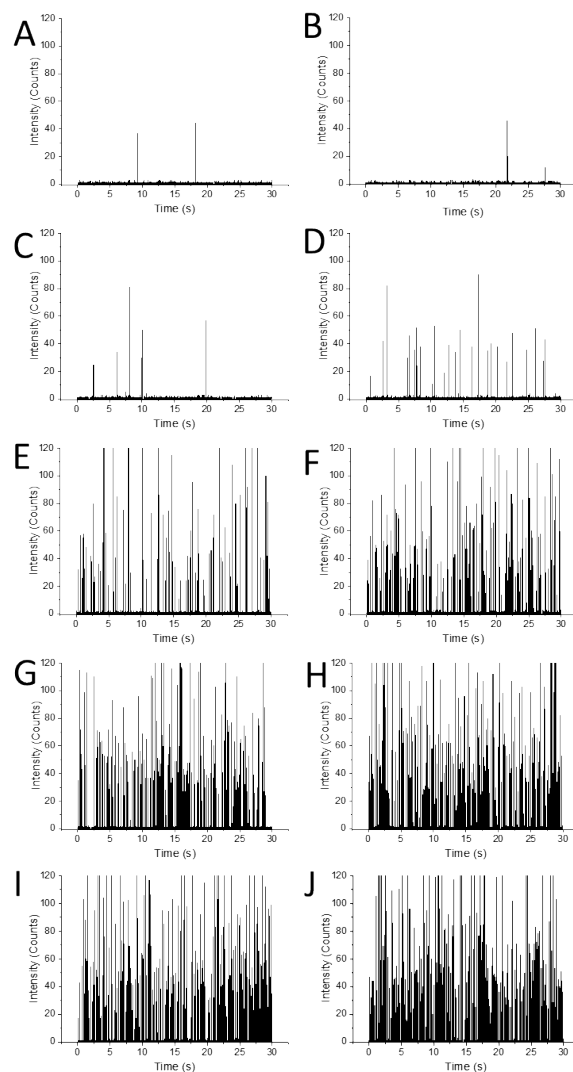


Figure 5. spICP-MS spectra of AuNPs in the presence of different concentrations of Thrombin (A to J: 0, 10^{-4} , 10^{-3} , 10^{-2} , 10^{-1} , 1, 10, 10^2 , 10^3 , 10^4 pM). GO/AuNPs composites concentration: 1 $\mu\text{g}/\text{mL}$ (GO mass based). Incubation at 37 $^{\circ}\text{C}$ for 60 min in PBS buffer (10 mM, 0.5 mM MgCl_2 , pH 7.4). 200 folds dilution before injecting into spICP-MS (^{197}Au , dwell time: 5 ms).

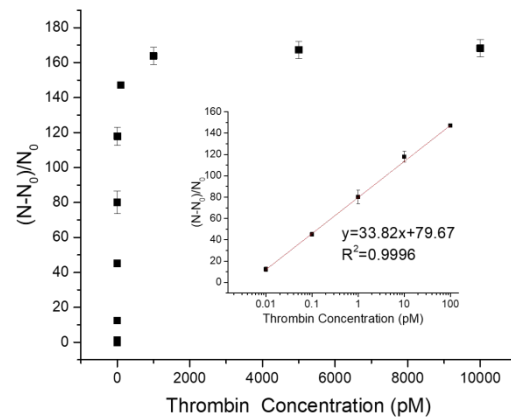


Figure 6. Relationship between the changes of number of detected AuNPs and thrombin in concentration from 10^{-4} to 10^4 pM. Acquisition period: 180 s. Inset: Calibration curve of the changes of number of detected AuNPs and thrombin concentration from 10^{-2} to 10^2 pM.

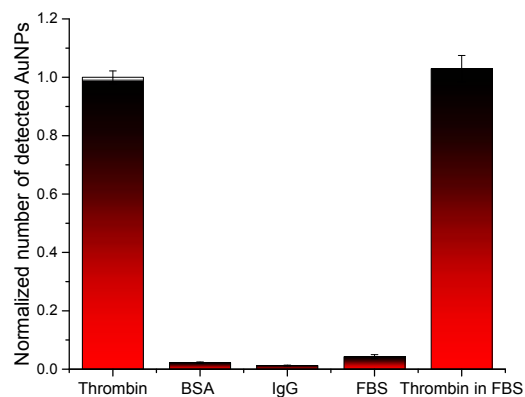
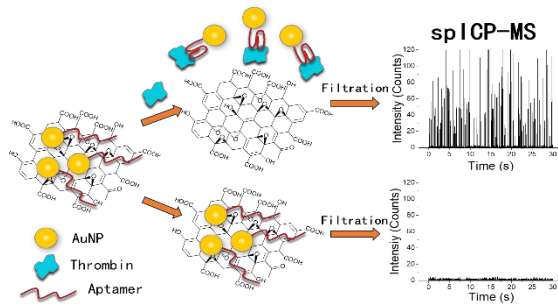


Figure 7. Selectivity of the platform for thrombin detection by spICP-MS. Thrombin concentration: 10.0 pM; BSA and IgG concentrations: 1.0 μ M; FBS concentration: \sim 0.1 g protein/L. GO/AuNPs composites concentration: 1 μ g/mL (GO mass based). Incubation at 37 $^{\circ}$ C for 60 min in PBS buffer (10 mM, 0.5 mM MgCl_2 , pH 7.4).



An ultrasensitive biomarker assay platform established by monitoring the gold nanoparticles (AuNPs) desorbed away from graphene triggered by target using single-particle inductively-coupled plasma/mass spectrometry (spICP-MS).